

BASIC BELL-MHD TURBULENCE

ANDREY BERESNYAK AND HUI LI
 Los Alamos National Laboratory, Los Alamos, NM 87545
Draft version June 6, 2014

ABSTRACT

Nonresonant current instability was identified by Bell (2004) as an important mechanism for magnetic field amplification in supernova remnants. In this paper we focus on studying the nonlinear stage of this instability using the incompressible MHD formulation. We demonstrate that the evolution of magnetic turbulence driven by the Bell instability resembles turbulence driven on large scales. More importantly, we demonstrate that the energy-containing scale for magnetic fields is proportional to the square root of the magnetic energy density. Given the observational constraints of the possible field amplification, this new relation allows us to directly estimate the maximum energy of particles scattered by such fields and this estimate is normally below the average particle energy. This implies that, without taking into account the feedback to cosmic rays, the typical scales of Bell fields, in either linear or nonlinear regime, will be too small to affect high energy particle acceleration. We mention several scenarios of back-reaction to cosmic rays that could be important.

1. INTRODUCTION

It has long been assumed on energetic arguments that SNRs are responsible for the acceleration of cosmic rays, at least up to the “Knee” of the spectrum at 10^{15} eV. The most common paradigm proposed for production of cosmic rays in supernova remnants is diffusive shock acceleration (DSA), in which particles scatter off magnetic turbulence and move across the shock multiple times (Krymskii 1977; Bell 1978; Blandford & Ostriker 1978). DSA produces an energy spectrum of E^{-2} , which is consistent with $E^{-2.7}$ power law observed at Earth, accounting for losses due to escape from the Galactic disk. The scattering rates in an ambient ISM magnetic field, however, are grossly insufficient to provide sizable acceleration and it has been argued that magnetic fields has to be amplified (Voelk et al. 1984; Blandford & Eichler 1987; Malkov & O’C Drury 2001). Thanks to the launch of Chandra X-ray Observatory, which had both the spatial resolution and sensitivity to map X-ray synchrotron emission from TeV electrons, magnetic field amplification has received observational support. Rather than a diffuse morphology, expected if the magnetic field were low and the Larmor radius of high-energy electrons were a significant fraction of the SNR diameter, the X-ray synchrotron emission in young SNRs is confined to a thin region near the shock front. This width, such as in the Cassiopeia A SNR, is interpreted as the post-shock distance traveled by a \sim TeV electron over a synchrotron cooling timescale (Vink & Laming 2003), which gives the inferred field strengths of $\sim 100\mu\text{G}$. Similar analysis in Tycho’s SNR gives around $300\mu\text{G}$ (Cassam-Chenaï et al. 2007). Evidence for magnetic field amplification, however, requires more detailed physical understanding.

One of the difficulties in creating a fully self-consistent theory of magnetic field amplification and cosmic ray acceleration is that it requires treatment of collisionless particles, e.g., CRs, as well as the background magnetized plasma, usually considered as MHD fluid. One of the popular approaches to capture the feedback of CRs on the MHD fluid is the so-called streaming instability,

where particles moving faster than Alfvénic speed amplify waves and confine themselves via scattering by the same resonant waves, see, e.g., Kulsrud & Pearce (1969); Lagage & Cesarsky (1983). Analytic linear models, however, can not deal with significant magnetic field amplification. While nonlinear models of streaming instability have already been suggested, e.g., by Diamond & Malkov (2007), their applicability is yet to be tested by CR-MHD simulations. In this situation a simplified approach, assuming that cosmic rays are acting on MHD plasma as an external current and that the bending of cosmic rays is small, was suggested by Bell (2004) and quickly gained popularity (see, e.g., Zirakashvili et al. 2008; Riquelme & Spitkovsky 2009; Bykov et al. 2011; Rogachevskii et al. 2012). Considering cosmic rays as a constant external current significantly simplifies the problem by bringing it to the realm of pure MHD, where large-scale nonlinear simulations have been a staple for many years.

While it is clear that most of the cosmic rays, except the highest energy ones, will be scattered many times over the lifetime of the supernova remnant, the local short-timescale treatment of cosmic rays as external current may indeed be useful. Over the years several important properties of Bell’s instability have been established on a qualitative level, e.g., it has been confirmed that the instability continues to grow after going into the nonlinear stage and that the mean scale of magnetic field also grows. One of the possibilities that has been investigated recently is the growth of large-scale fields either due to kinetic mechanisms (Bykov et al. 2011), which appealed to the oblique instability that would grow slower or on much larger scales or due to the large-scale dynamo (Rogachevskii et al. 2012), which would again result in slower exponential growth of the magnetic field on larger scales.

In this paper we present the study of linear and nonlinear stages of Bell’s instability in one of the simplest possible setups – incompressible MHD equations driven by constant external current density. The simplicity of our approach highlights the symmetries of MHD equations

and allowed us to achieve a simple physical understanding of the nonlinear stage. In particular we predict a simple law of growth for the magnetic outer scale, which is of primary importance to determine if the Bell instability can generate magnetic fields which could scatter high-energy particles. Our answer to the above riddle seems to be negative. Despite the fact that the magnetic outer scale grows very quickly, so does the magnetic energy density. Furthermore, they seem to be connected by a universal relation, and, at the levels of magnetic saturation brought by energetic or observational grounds (Bell 2004; Völk et al. 2005), we don't expect this magnetic field to be important for scattering.

This paper is organized as follows: Section 1 describes MHD equations driven by external currents and overviews the global conservation properties and the physical source of energy that drives the turbulence. Section 2 suggests a simple model for the nonlinear stage of the instability, inspired by extending linear model to the case when magnetic field is randomly oriented with respect to the external current. Section 3 presents our numerical results, compares them with the predictions of the model and determines dimensionless coefficients introduced by the model. Section 4 is devoted to the discussion of astrophysical implications of the current work.

2. BELL-MHD EQUATIONS AND CONSERVATION LAWS

Assuming that cosmic rays have very high energy and do not efficiently interact with the MHD fluid, Bell (2004) suggested that the portion of the Lorentz force, associated with the cosmic ray current should be subtracted from the total Lorentz force, as this portion is not applied directly to the fluid. The induction equation, however, is unchanged, as it is the consequence of the Ohm's law. The resulting equations are MHD equations with an external current, which we call Bell-MHD equations¹:

$$(\partial_t + \mathbf{v} \cdot \nabla) \mathbf{v} = -\nabla P + \mathbf{j} \times \mathbf{B} - \mathbf{j}_e \times \mathbf{B}, \quad (1)$$

$$\partial_t \mathbf{B} = \nabla \times (\mathbf{v} \times \mathbf{B}). \quad (2)$$

The equations above are basically MHD equations with an extra "force" $-\mathbf{j}_e \times \mathbf{B}$. Physically this extra term means that the MHD fluid has external current embedded in it, which has an electric connection with a fluid, but does not apply any force to the fluid. A certain insight into the dynamics could be obtained by reviewing conservation laws for the above system. Originally, MHD equations have five basic conservation laws for scalar or pseudoscalar quantities: mass m , momentum p , energy E , cross-helicity H_c and magnetic helicity H_M . As the continuity equation is unchanged, it is easy to verify that conservation of mass still holds. Furthermore, as induction equation is unchanged, the magnetic helicity conser-

¹ Here we used Heaviside-Alfvén units with $\mathbf{j} = \nabla \times \mathbf{B}$, which avoid having a factors of $\sqrt{4\pi}$, ρ and c in the MHD equations and also expresses the magnetic field in velocity units, as the density assumed to be unity. It is easy to go back to CGS units remembering that energy density in Heaviside-Alfvén units is $\rho(B^2 + v^2)/2$. Also, the current density $j = (j_{\text{CGS}}/c)(4\pi/\rho)^{1/2}$. These units allow us to concentrate on the physics of the instability and keep the narrative compact. They are also a great choice for units in the numerical studies of incompressible MHD.

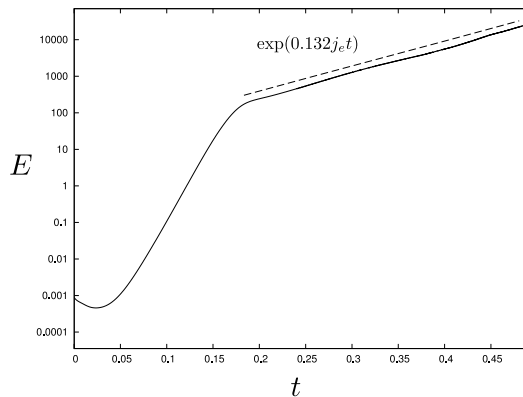


FIG. 1.— Energy grows exponentially in both linear and nonlinear regime of Bell's instability. While the linear growth rate is approximately j_e , the nonlinear growth rate is reduced by a factor of 0.132.

vation still holds and multiplying Eq. 1 by \mathbf{B} we can verify that cross-helicity is also conserved. The two conservation laws that are broken by the Bell-MHD system are the energy and momentum conservation. The average extra momentum per unit time is related to the average magnetic field \mathbf{B}_0 as $-\mathbf{j}_e \times \mathbf{B}_0$. This extra momentum has to be provided by external currents. In the case of supernova remnants, the amount of momentum carried by high energy cosmic rays is small compared to the inflowing fluid momentum, therefore the component of external currents which is perpendicular to \mathbf{B}_0 will be suppressed in one gyration for the current-carrying cosmic rays. Keeping in mind of this, we will consider only the case when $\mathbf{j}_e \parallel \mathbf{B}_0$ and the global momentum conservation holds true. Multiplying Eq. 1 by \mathbf{v} we see that the extra energy per unit time is $-\mathbf{v} \cdot (\mathbf{j}_e \times \mathbf{B}) = \mathbf{j}_e \cdot (\mathbf{v} \times \mathbf{B})$, i.e. it is associated with the electromotive force (EMF) of the fluid, $\mathcal{E} = \mathbf{v} \times \mathbf{B}$, applied to the external current. As we'll see below for the unstable modes, MHD fluid applies such an EMF as to extract energy from the external current. Obviously, this results in energy loss in the loop of the external current. In the case of the external current provided by cosmic rays, they are being slowed down by MHD fluid's EMF. We can also write down Eq. 1 in Fourier space and investigate energy injection as a function of scale. In order to do this, the equations for the time derivative of the Fourier-transformed velocity \hat{v}_k have to be multiplied to \hat{v}_k^* , a complex conjugate. The result is the energy injection with the rate of $\mathbf{j}_e \cdot (\mathbf{v}_k \times \mathbf{B}_k^*)$, or $\mathbf{j}_e \cdot \mathcal{E}_k$, where \mathcal{E}_k is the power spectrum of EMF, $(\mathbf{v}_k \times \mathbf{B}_k^*)$.

3. LINEAR AND NONLINEAR STAGES

The linear stage of Bell's instability can be investigated by applying small perturbations to the initial state $\mathbf{B} = \mathbf{B}_0$. This initial state corresponds to plasma current completely canceling out the external current, i.e. the total current of zero. The mutual repulsion of external and plasma current results in an unstable situation which will grow exponentially from small perturbations of \mathbf{B}_1 and \mathbf{v}_1 . Using linear analysis of the equations above one can verify that the fastest growing mode has a wavenumber $k_d = j_e/2B_0$ parallel to \mathbf{B}_0 , while the perturbations \mathbf{B}_1 and \mathbf{v}_1 are perpendicular to \mathbf{B}_0 and have

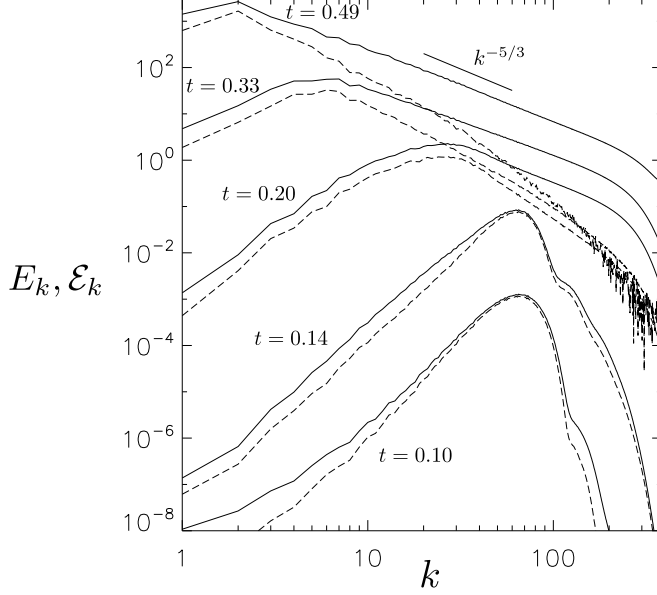


FIG. 2.— Energy spectra (solid) and EMF spectra (dashed) at several moments of simulation time. We only take the vector component of EMF which is parallel to j_e , therefore the dashed spectrum is also the energy injection spectrum. First two spectra feature linear mode growth with EMF spectrum proportional to the energy spectrum. Later, nonlinear stages show EMF driving dominant at the largest, energy containing scale of the spectrum. Below energy-containing scale the energy injection becomes negligible and the spectrum exhibiting an “inertial range” $k^{-5/3}$ scaling. The approximate Kolmogorov scaling in the nonlinear regime was reported earlier by Rogachevskii et al. (2012).

a certain sign of circular polarization, corresponding to the sign of current helicity $\mathbf{j}_e \cdot \mathbf{B}_0$ (Bell 2004). Energy is equipartitioned between \mathbf{v} and \mathbf{B} . The fastest growing mode of field perturbations grows at the rate² of $j_e/2$, while the energy grows at a rate j_e . It is also worth noting that in the presence of scalar viscosity ν and magnetic diffusivity ν_m this growth rate will be decreased by $-(\nu + \nu_m)j_e^2/4B_0^2$.

The nonlinear stage takes over when nonlinear terms of Eqs. (1-2) become comparable with linear terms. This will happen when energy density exceeds characteristic initial energy density $B_0^2/2$. Note that in the limit of ideal incompressible MHD statistically homogeneous system described by Eqs. (1)-(2) has a single characteristic energy density scale, B_0^2 , timescale $1/j_e$, which corresponds to the linear growth rate, and lengthscale B_0/j_e , which corresponds to the wavelength of the most unstable mode. If we conjecture that B_0 will become unimportant later in the nonlinear evolution, the system will only have a characteristic timescale $1/j_e$. It also turns out that dissipative effects can be neglected as long as B_0/j_e is above all dissipative scales.

Suppose at some moment of time during nonlinear evolution the spectrum of perturbations has an integral (outer) scale L . We will argue that perturbations on this scale will be able to freely expand due to the Lorentz force, just like an unstable helical mode in the linear regime. We will also conjecture, by analogy with lin-

² In CGS units $k_d(\text{CGS}) = 4\pi j_e(\text{CGS})/(2B_0 c)$ and the growth rate is $(j_e(\text{CGS})/2c)(4\pi/\rho)^{1/2}$.

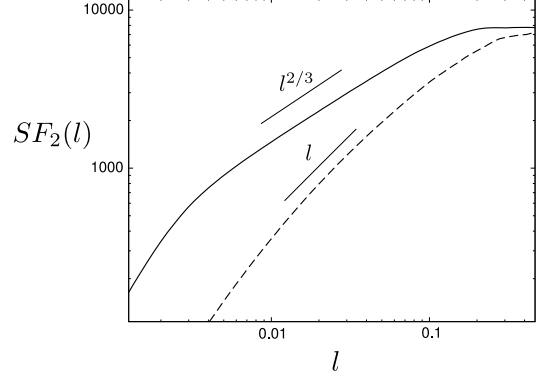


FIG. 3.— Anisotropy of Bell-MHD turbulence below the energy containing scale at $t = 0.49$. In this plot we show second order structure functions of density parallel (dashed) and perpendicular (solid) to the local mean magnetic field. The scalings of l^1 and $l^{2/3}$ are expected from inertial range of strong MHD turbulence Goldreich & Sridhar (1995). Our measurement is grossly consistent with the Goldreich-Sridhar anisotropy.

ear stage, that the product $\mathbf{j}_e \cdot (\mathbf{v} \times \mathbf{B})$, i.e. the work of external current onto the fluid, will be proportional to energy. The difference with the linear stage is that the EMF spectrum will no longer be proportional to the energy spectrum, rather it will peak at the integral scale. The result will be the growth of energy at the integral scale, the growth of the integral scale itself and the direct energy cascade on scales below integral scale. From here on we introduce two dimensionless constants that describe this process: the ratio of EMF to total energy (which conventionally have the same Heaviside-Alfvén units) C_E and the fraction of energy that goes into the direct cascade C_D . We expect C_E and C_D to be below unity. The whole spectrum of perturbations at any moment of time will be determined only by the total energy E and the integral scale L . The time evolution for these will be determined by

$$\frac{dE}{dt} = (1 - C_D)C_E j_e E. \quad (3)$$

At the same time the zeroth law of turbulence, which states that at the sufficiently high Reynolds numbers³ the dissipation will only depend on large-scale quantities, will read:

$$\frac{E^{3/2}}{L} = C_K C_D C_E j_e E. \quad (4)$$

Here we have introduced Kolmogorov constant C_K . This will eventually give us the relation between the integral scale and the energy density:

$$L = E^{3/2}/(C_K C_D C_E j_e E) = E^{1/2}/(C_K C_D C_E j_e). \quad (5)$$

³ This condition, in our case, will be satisfied as long as the dissipation scales are much smaller than all relevant scales of the problem, including $1/k_d = B_0/j_e$. Given the expressions below, it is easy to show that as long as $\nu, \nu_m < B_0^2/j_e$, i.e. there is a positive growth rate in the linear regime, the dissipation scale will be smaller than $1/k_d(B_0/B)^{1/2}$, i.e. this condition is always satisfied as long as there is a growth of instability. Naturally, the small but finite dissipation effects are required for the turbulent cascade to terminate and produce heat.

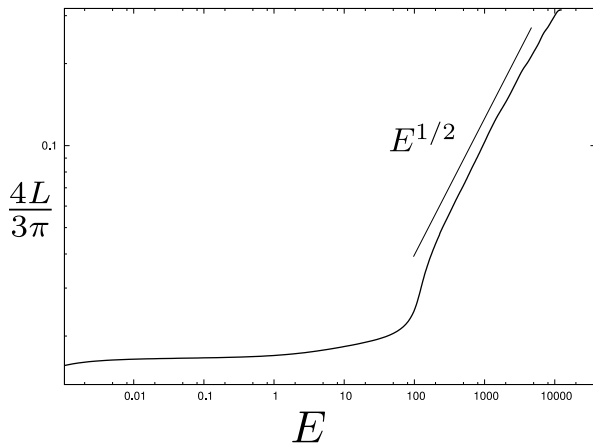


FIG. 4.— The dependence of energy containing scale L on energy density E . The linear growth regime features constant L , corresponding to the wavelength of the fastest growing mode. The nonlinear regime is characterized by the $l \sim E^{1/2}$ law, with both E and l growing exponentially in time. Outer scale L is defined through spectrum as $(3\pi/4) \int k^{-1} E(k) dk / E$ (Gotoh et al. 2002).

Since we expect equipartition between magnetic and kinetic energies, Eq. (5) has a simple physical meaning. Since $E^{1/2} \sim B$, the fluctuations of the magnetic field are such that the fluctuations of the total current density (plasma plus external) are of the order of the external current density itself, on the outer scale of turbulence. In other words, collisions of expanding spirals from Bell instability almost fully randomizes total current, but its RMS value always stay around j_e .

The scalings above could be verified in numerics, in particular we observe that the energy density clearly continues to grow exponentially in the nonlinear stage, Fig. 1. And the outer scale L indeed follows the above scaling (see Fig. 4). We can also directly verify that EMF drives turbulence mostly on the integral scale.

One of the possibilities brought up recently by Rogachevskii et al. (2012) is that since the original Bell's instability generates helical states, the kinetic helicity of the resulting turbulence will amplify any large-scale field on scale l , roughly at a rate α/l , where α is due to the α -effect of helical turbulence. Our model does not explicitly deal with helicities, however it assumes that the mechanism of growth is essentially the same as in the linear regime – i.e. the expanding magnetic helices. The difference is that this time the sign of helicity is determined by mutual orientation of j_e and the local field, which becomes increasingly isotropic as B_0 becomes energetically unimportant. In other words, we expect global fractional kinetic helicity to go to zero and the largest fluctuations of helicity only present on the outer scale of turbulence L . Our conclusion, therefore, does not directly challenge the statement of Rogachevskii et al. (2012) but amends it by saying that the growth of the field on scales which are much larger than L is suppressed due to kinetic helicity being averaged-out on such scales.

4. NUMERICS

We performed a series of numerical experiments to verify and refine the hypotheses stated above. We used incompressible pseudospectral code which solves Eqs. (1-2) with extra dissipation terms which are used to regularize

numerical solution. For dissipation terms we used hyperdiffusivity of fourth order, equal in both v and B , purely out of convenience: 1) the hyperdiffusivities allowed us to push k_d closer to the Nyquist frequency k_N without affecting linear growth rate too much, typically we used $k_d \approx 0.1k_N$. This allowed us to have greater scale separation between the box size and $1/k_d$ to study self-similar nonlinear behavior for a greater range of scales and energies; 2) the dissipation rate varied by several orders of magnitude during the simulation and having second-order diffusivities would have required constantly tuning diffusion coefficients to keep the simulation well-resolved. Regarding further details of the code architecture, accuracy and implementation we refer to our previous publications, e.g. Beresnyak & Lazarian (2009). It is also worth noting that the code preserved scaling symmetries of the incompressible MHD equations, e.g. rescaling time in proportion with $1/j_e$, while keeping j_e/B_0 constant would result in exactly the same evolution.

We performed a series of six 384^3 experiments changing the value of initial magnetic field B_0 between values of 0.5, 1.0 and 2.0 and changing current between 40 and 20. Due to the symmetries of the dynamical equations, we expected simulations with the same j_e/B_0 ratio to exhibit the same behavior, assuming that the timescale was properly rescaled to $1/j_e$. This was indeed the case. Also, as long as the scale $1/k_d$ was well separated from both dissipation scale and the cube size scale, the behaviour was similar for all simulations, assuming the same rescaling. Due to the fact that incompressible MHD are scale-free, the only true physical parameter of the problem is j_e and since it has units of $1/s$, it simply designates the only available timescale for the problem. In other words, the evolution is expected to be universal as long as the dissipation coefficients are small and the box size is large enough. Keeping this in mind we performed a single 1152^3 large-scale simulation to verify the scaling in Eq. (5). In this simulation we chose $j_e = 120$, $B_0 = 1$, so that $k_d = 60$ and is well-separated from dissipation scale at around $k = 300$. Figures 1-5 present measurements from this simulation. The total energy evolution is presented on Fig. 1, while spectra of total energy and the EMF along j_e are presented on Fig. 2. A few comments on these results are in order. First of all, the nonlinear regime exhibits a pure exponential growth, over at least a couple of order of magnitude in energy, which is fully consistent with our model and implicitly verifies that the external current density j_e determines the only relevant timescale of the problem. The coefficient of reduction of the growth rate, 0.132, that we conjectured to be equal to the $(1 - C_D)C_E$ product indeed seems to be universal among several simulations with different j_e , B_0 and numerical resolutions. We observe the transition to nonlinear stage at approximately the same level of $B_{\text{rms}}/B_0 \sim 10$ as previous simulations, e.g., Rogachevskii et al. (2012).

Furthermore, the spectra of energy and EMF, Fig. 2, seem to support our conjectures about the scales at which the Bell-MHD turbulence is driven. For the linear growth regime, represented on Fig. 2 by spectra at $t=0.1$ and $t=0.14$, the driving EMF spectrum is basically proportional to the energy spectrum, while for nonlinear growth regime at $t=0.2$, 0.33 and 0.49 the EMF is peaked on the outer scale, supporting our conjecture

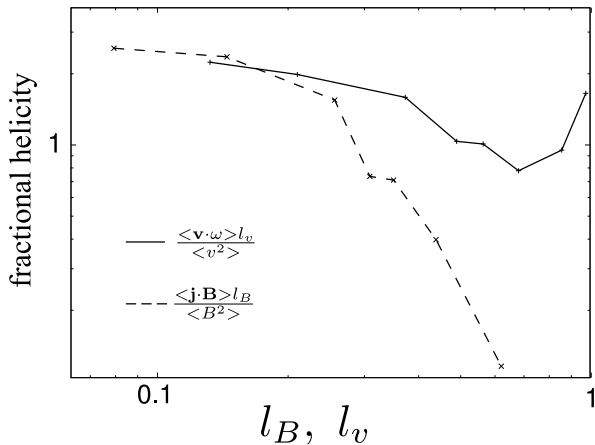


FIG. 5.— Fractional kinetic helicity vs kinetic scale (solid) and fractional current helicity vs magnetic scale (dashed). While fractional kinetic and current helicities are large in the linear mode growth, they decrease during nonlinear growth, which is due to randomization of magnetic field direction with respect to the external current direction. When the other scale L approaches the box size, however, the kinetic helicity starts growing again, while current helicity changes sign.

about large-scale driving. In fact, in order to be important on smaller scales l and to interfere with the energy cascade through scales the EMF has to be at least scale-independent or to grow with smaller scales, which is clearly not the case. From the reduced ratio of EMF to energy in the nonlinear regime, we derive $C_E \approx 0.58$ and using $(1 - C_D)C_E = 0.132$ we have the fraction of energy captured by the direct cascade and dissipated as $C_D = 0.77$.

It is also interesting to study the statistical properties of the nonlinear Bell-MHD turbulence and see if they are similar to the ordinary direct-cascade MHD turbulence driven on large scales. We measured second-order structure function $SF(l)$ parallel and perpendicular to the local magnetic field, which are supposed to scale as l and $l^{2/3}$ correspondingly, according to the standard model of strong MHD turbulence by Goldreich & Sridhar (1995). We found that the structure function measurement grossly consistent with the theory, see Fig. 3. One of the important consequences of this is that due to local anisotropy, the Bell-generated turbulence will be inefficient at scattering particles with gyroradii much smaller than the outer scale L , see, e.g., Chandran (2000); Yan & Lazarian (2002), just like the driven MHD turbulence.

As the instability enters the nonlinear stage, the outer scale quickly grows, in fact, exponentially in time. Fig. 4 investigates the dependence of the outer scale on the mean energy density and finds that indeed outer scale grows as the square root of energy density as Eq. (5) suggests. We found that $L \approx 0.97E^{1/2}/j_e$. Assuming equipartition between magnetic and kinetic energies which is indeed approximately satisfied, and going back to CGS units in the above relation, we obtain $B_{\text{rms}}(\text{CGS}) \approx 4\pi j_e(\text{CGS})L(\text{CGS})/c$.

Let us discuss the role of kinetic and current helicities. Starting with the linear stage of the instability, when the plasma current equals approximately $-\mathbf{j}_e$, the system has large current helicity $-\mathbf{j}_e \cdot \mathbf{B}_0$ and the linearly growing

mode also has large kinetic helicity of the same sign. As the instability enters the nonlinear stage, however, one would expect that the influence of the mean field B_0 will decrease. The helical term $-\mathbf{j}_e \cdot \mathbf{B}_0$ will be relatively less important at later stages of the nonlinear evolution, while the fluctuating $-\mathbf{j}_e \cdot \mathbf{B}(\mathbf{r})$ will be more important. At each snapshot of the nonlinear evolution, given the outer scale of Bell turbulence $L(t)$ at this time, the most contribution to both the energy growth and kinetic and current helicities will come from scale $L(t)$ because the scales below $L(t)$ represent direct cascade. However, averaged over the system size, which is expected to be much larger than $L(t)$, the total helicity should be relatively small, as at the each eddy of size $L(t)$ the helical terms are determined by randomly oriented $-\mathbf{j}_e \cdot \mathbf{B}(\mathbf{r})$. The high local kinetic helicity on scale $L(t)$, therefore, will result in a growth of larger scale field on the next available largest scale, figuratively speaking $2L(t)$, but will not result in a growth on much larger scales, because at those scales the $-\mathbf{j}_e \cdot \mathbf{B}(\mathbf{r})$ is randomized.

In order to check this hypothesis we calculated global kinetic and current helicities as a function of time. Fig. 5 shows dimensionless fractional helicities as a function of magnetic and kinetic scale. While in the linear stage $-\mathbf{j}_e \cdot \mathbf{B}_0$ term is dominant and both fractional current and kinetic helicities are large, as the instability progresses to larger scales, global fractional helicities decrease. This is because the large helicities produced locally on scale L are of random sign and are averaged out on the scale of the box. It is interesting, however, that when the outer scale L approached the box size the fractional kinetic helicity started growing again. We believe that when the system reaches the box size it chooses the dominant global helical state and sticks to it. As we believe that the supernova precursor size is always much larger than the outer scale L , this should be interpreted as an artificial numerical effect, associated with the finite box size.

Lastly, to further challenge the idea of prevalent influence of initial current helicity, we investigated the case with zero mean field B_0 . This situation is special in a sense that the system did not have any preferred helicity to begin with. The instability, therefore has to grow starting with low-level magnetic noise with which we seeded the simulation. In this case the fast linear growth was not observed, however, after some period of slower growth the simulation entered nonlinear stage. In this nonlinear stage the growth rate was consistent with $0.132j_e$, the same rate that we observed in the nonlinear stage of all helical cases.

5. DISCUSSION

Our estimate of outer scale Eq. (5) can be readily converted to the estimates of the maximum energy of accelerated particles, assuming that current is due to all CRs drifting with the average speed of the shock v_s :

$$E_{\text{max}} = \frac{v_s}{c} e B_{\text{rms}} L \approx \frac{B_{\text{rms}}^2}{4\pi n_{\text{CR}}} \quad (6)$$

That is, the *maximum* particle energy equals to the average magnetic energy per particle. The estimate of maximum magnetic energy density in terms of cosmic ray energy density U_{CR} was given by Bell (2004) as $(v_s/c)U_{\text{CR}}$. Using this estimate we get $E_{\text{max}} = 2(v_s/c)U_{\text{CR}}/n_{\text{CR}}$,

i.e. E_{\max} is much smaller than the average cosmic ray energy. The estimate of Völk et al. (2005) gives $B_{\text{rms}}^2/(8\pi) = 1.7 \times 10^{-2} \rho v_s^2$, based on observational data. Using this estimate and assuming that $U_{\text{CR}} = 10^{-1} \rho v_s^2$, $E_{\max} = 0.34 U_{\text{CR}}/n_{\text{CR}}$. The average energy of CRs $U_{\text{CR}}/n_{\text{CR}}$ is expected to be low, around 1 GeV, however in any case it should be lower than maximum energy, not vice versa. Furthermore, if we assume that some of the current is due to cosmic rays escaping with a speed of light, i.e. $j_e > ev_s n_{\text{CR}}$ our estimate of E_{\max} will be even lower, somewhat counter-intuitively, because our Eq. (5) suggests that the saturation scale of L will be inversely proportional to j_e . All in all, assuming that classic Bell's mechanism increases maximum energy of accelerated particles, we came to a contradiction⁴. It seems that without considering the feedback of magnetic perturbations on cosmic rays, using just classic current instability will not result in decreased diffusion of cosmic rays on the high-energy end. When considering feedback, however, treating cosmic rays as homogeneous current is not sufficient and gyroresonance effects should be included.

Let us compare the $L \sim E^{1/2}$ dependence produced by Bell's mechanism with other magnetic field generation mechanisms. The small-scale dynamo have a $L \sim E^{3/2}$ dependence, with E being the energy density of the magnetic field (Beresnyak 2012), thus for these two mechanisms the product of LB , which determines the scattering of highest energy particles, will be E^1 and E^2 correspondingly. Given that the magnetic energy density E is bound on energetic grounds, and also constrained by observations (Vink & Laming 2003; Cassam-Chenaï et al. 2007; Völk et al. 2005), the $LB \sim E^2$ seems more favorable than $LB \sim E$.

Prior numerical work investigating linear and nonlinear stages of Bell's instability includes Bell (2004); Zirakashvili et al. (2008); Riquelme & Spitkovsky (2009); Rogachevskii et al. (2012). Transition to the nonlinear regime has happened at about the same level of perturbations in Bell (2004); Zirakashvili et al. (2008); Rogachevskii et al. (2012) and this investigation. All fluid simulations have shown some growth at the nonlinear stage, but the exponential nature of this growth was less evident compared to our Fig 1. The above simulations were interpreted in various ways using phenomenological argumentation. For example, Bell (2004) suggested that the magnetic spectrum will be defined by scale-wise equilibrium of magnetic tension, which will result in a power spectrum of k^{-3} . Rogachevskii et al. (2012) noticed that the spectrum is shallower than that, around $-5/3$, due to the presence

⁴ In the Equation (6) we used the condition of efficient scattering for high energy particles, so that the Larmor radius r_L should be smaller than $v_s L/c$. We do not expect the cosmic rays precursor to be much thicker than L in the pure Bell instability case, because the precursor thickness will be determined by the saturation of the instability itself and the efficient scattering of low-energy particle that should happen on scales smaller than L . However, if one believes that the Bell-CR precursor is much thicker, one may use the other formula for the scattering rate for the case $r_L \gg L$. This should give the maximum larmor radius of accelerated particles as $r_{\max} = (v_s L_p L/c)^{1/2}$, where L_p is the precursor thickness. However, assuming maximum field strength of $100 \mu\text{G}$, even fairly large $L_p \approx 0.1 \text{ pc}$ still gives maximum energies of around 2 TeV, way below the knee of the CR spectrum.

of the direct cascade. While all of the above papers mention the growth of the outer scale in the nonlinear regime, only Rogachevskii et al. (2012) made quantitative predictions regarding such growth. This paper was the first to measure anisotropy in Bell-MHD turbulence. Plasma simulations of Riquelme & Spitkovsky (2009) qualitatively confirmed current instability and identified some differences compared to the fluid case. The detailed comparison with this paper would be outside the scope of this presentation.

The key properties of the Bell-MHD turbulence we have uncovered, such as Eq. (5) suggest that, when considering including the feedback on cosmic rays and/or making conjectures about their possible roles in cosmic ray acceleration, one has to be very careful in adopting the spectrum and amplitude of such turbulence. This is because this turbulence will strongly affect the properties of lower-energy CRs, i.e. the same particles that mostly contribute to current. Another source of uncertainty would be understanding possible effects of compressible turbulence. Our picture of growing magnetic helices on the outer scale L due to interaction with local external current does not explicitly depend on fluid pressure, however, and the zeroth law of turbulence Eq. (4), to the best of our knowledge, is supposed to be correct even in supersonic turbulence. Furthermore, since our results indicate that the C_D fraction of total energy goes into the direct cascade and dissipates into heat, the sonic Mach number of Bell-MHD turbulence can be estimated as $M_s \approx \sqrt{(1 - C_D)/2C_D} \approx 0.4$. Although qualitatively the picture of nonlinear stage is not supposed to change, we might expect the coefficients C_D , C_E and C_K to somewhat vary in the compressible case.

Our results are applicable not only to supernova remnants problem, but to any conductive fluid with external current, e.g., plasma with rigid wires embedded in it and the current driven by an external voltage. The quick exponential growth of both energy and fluid EMF suggests that external energy source will only be able to maintain such current for a limited amount of time.

Several pathways are available to study back-reaction to cosmic rays. One of the approaches is the bottom-up plasma simulations, e.g., by Riquelme & Spitkovsky (2009) who tried to capture scaling behaviours that may be extended to larger scales. The full treatment of nonlinear streaming instability (Diamond & Malkov 2007) is the most general and desired approach, but has significant analytical difficulties. The path to explore the long wavelength dynamics while keeping Bell's instability intact (Bykov et al. 2011; Rogachevskii et al. 2012) has also been popular recently. The entirely different approach to get turbulence driven on large scales by pre-existing density inhomogeneities and the non-barotropic cosmic ray pressure was suggested in Beresnyak et al. (2009) and currently being pursued by Drury & Downes (2012); Brüggén (2013) and the authors of this paper. We believe that large-scale three-dimensional MHD-particle simulations could shed light on this extremely complex theoretical problem.

6. ACKNOWLEDGMENTS

AB is grateful to Mischa Malkov, Axel Brandenburg, Tony Bell, Vladimir Zirakashvili, Pat Diamond and Alex Schekochihin for useful discussions. The work

is supported by the LANL/LDRD program and the DoE/Office of Fusion Energy Sciences through CMSO. Computing resources at LANL are provided through the

Institutional Computing Program.

REFERENCES

- Bell, A. R. 1978, *MNRAS* , 182, 147
 —. 2004, *MNRAS* , 353, 550
 Beresnyak, A. 2012, *Phys. Rev. Lett.*, 108, 035002
 Beresnyak, A., Jones, T. W., & Lazarian, A. 2009, *ApJ*, 707, 1541
 Beresnyak, A., & Lazarian, A. 2009, *ApJ*, 702, 460
 Blandford, R., & Eichler, D. 1987, *Phys. Rep.* , 154, 1
 Blandford, R. D., & Ostriker, J. P. 1978, *ApJ* , 221, L29
 Brüggén, M. 2013, *MNRAS* , 436, 294
 Bykov, A. M., Osipov, S. M., & Ellison, D. C. 2011, *MNRAS* , 410, 39
 Cassam-Chenaï, G., Hughes, J. P., Ballet, J., & Decourchelle, A. 2007, *ApJ*, 665, 315
 Chandran, B. D. G. 2000, *Physical Review Letters*, 85, 4656
 Diamond, P. H., & Malkov, M. A. 2007, *ApJ*, 654, 252
 Drury, L. O., & Downes, T. P. 2012, *MNRAS* , 427, 2308
 Goldreich, P., & Sridhar, S. 1995, *ApJ*, 438, 763
 Gotoh, T., Fukayama, D., & Nakano, T. 2002, *Physics of Fluids*, 14, 1065
 Krymskii, G. F. 1977, *Soviet Physics Doklady*, 22, 327
 Kulsrud, R., & Pearce, W. P. 1969, *ApJ*, 156, 445
 Lagage, P. O., & Cesarsky, C. J. 1983, *A&A* , 125, 249
 Malkov, M. A., & O’C Drury, L. 2001, *Reports on Progress in Physics*, 64, 429
 Riquelme, M. A., & Spitkovsky, A. 2009, *ApJ*, 694, 626
 Rogachevskii, I., Kleeorin, N., Brandenburg, A., & Eichler, D. 2012, *ApJ*, 753, 6
 Vink, J., & Laming, J. M. 2003, *ApJ*, 584, 758
 Voelk, H. J., Drury, L. O., & McKenzie, J. F. 1984, *A&A* , 130, 19
 Völk, H. J., Berezhko, E. G., & Ksenofontov, L. T. 2005, *A&A* , 433, 229
 Yan, H., & Lazarian, A. 2002, *Phys. Rev. Lett.*, 89, B1102
 Zirakashvili, V. N., Ptuskin, V. S., & Völk, H. J. 2008, *ApJ*, 678, 255